Oncology Research, Vol. 28, pp. 273–284
Printed in the USA.

0965-0407/20 $90.00 + .00
DOI: https://doi.org/10.3727/096504020X15783052025051
E-ISSN 1555-3906
www.cognizantcommunication.com

Fzd2 Contributes to Breast Cancer Cell Mesenchymal-Like Stemness and Drug Resistance

Ping Yin,* Wei Wang,* Jian Gao,† Yu Bai,* Zhuo Wang,* Lei Na,* Yu Sun,* and Chenghai Zhao*

*Department of Pathophysiology, College of Basic Medical Science, China Medical University, Shenyang, China
†Center of Laboratory Technology and Experimental Medicine, China Medical University, Shengyang, China

Cancer cell stemness is responsible for cancer relapse, distal metastasis, and drug resistance. Here we identified that Frizzled 2 (Fzd2), one member of Wnt receptor Frizzled family, induced human breast cancer (BC) cell stemness via noncanonical Wnt pathways. Fzd2 was overexpressed in human BC tissues, and Fzd2 overexpression was associated with an unfavorable outcome. Fzd2 knockdown (KD) disturbed the mesenchymal-like phenotype, migration, and invasion of BC cells. Moreover, Fzd2 KD impaired BC cell mammosphere formation, reduced $Lgr5^+$ BC cell subpopulation, and enhanced sensitivity of BC cells to chemical agents. Mechanistically, Fzd2 modulated and bound with Wnt5a/b and Wnt3 to activate several oncogenic pathways such as interleukin-6 (IL-6)/Stat3, Yes-associated protein 1 (Yap1), and transforming growth factor-β1 (TGF-β1)/Smad3. These data indicate that Fzd2 contributes to BC cell mesenchymal-like stemness; targeting Fzd2 may inhibit BC recurrence, metastasis, and chemoresistance.

Key words: Frizzled 2 (Fzd2); Mesenchymal-like stemness; Lgr5; Drug resistance; Wnt

INTRODUCTION

Studies on transgenic animals such as MMTV-*WNT1*, MMTV-*βCATΔN*, and MMTV-*WNT10B* mice have demonstrated that overactivation of canonical Wnt/β-catenin signaling can induce breast cancer (BC) development[1]. Some components in this pathway including Wnt10b, Frizzled 7 (Fzd7), and low-density lipoprotein (LDL) receptor-related proteins 6 (LRP6) are associated with human BC, especially triple-negative BC (TNBC) or basal-like BC (BLBC)[2–4]. Wnt/β-catenin signaling promotes BC metastasis and chemoresistance, mostly due to the induction of epithelial–mesenchymal transition (EMT) and stem cell-like properties (also known as stemness). However, roles of noncanonical Wnt pathways in human BC are not completely understood. Wnt5a has been identified as both tumor suppressor and tumor promoter[5,6]. The discrepancy may be related to cellular context and receptor type[7,8].

Stemness induces cancer initiation, metastasis, recurrence, and chemoresistance. Two types of stemness, mesenchymal-like and epithelial-like, have been observed in BC cells[9]. Mesenchymal-like stemness is characterized by EMT, while epithelial-like stemness is characterized by its reverse process, mesenchymal–epithelial transition (MET). EMT links mesenchymal-like stemness to tumor-initiating capacity through several molecules such as RAS, p53, vascular endothelial growth factor (VEGF), Hedgehog, and transforming growth factor-β (TGF-β)[10–14].

Fzd proteins are seven-transmembrane receptors for Wnt ligands. Until now, 10 Fzd (Fzd1–Fzd10) have been identified. Fzd7 promotes TNBC proliferation and invasion through canonical β-catenin pathway[15], and Fzd6 induces TNBC invasion and metastasis by modulating actin cytoskeleton[16]. Roles of other Fzd in BC remain largely unknown. Our study revealed that Fzd2 modulates and binds with Wnt5a/b and Wnt3 to activate several oncogenic pathways and endow BC cell with mesenchymal-like stemness.

MATERIALS AND METHODS

In Silico Analysis

The Cancer Genome Atlas (TCGA) database was interrogated for *FZD2* expression in BC tissues. Cancer Cell Line Encyclopedia (CCLE) database and GSE12777 database were interrogated for gene expression in human BC

Address correspondence to Chenghai Zhao, Department of Pathophysiology, College of Basic Medical Science, China Medical University, No. 77 Puhe Road, Shenyang North New Area, Shenyang, Liaoning Province, P.R. China. Tel: 86+24+31939318; E-mail: chzhao@cmu.edu.cn

cell lines. Correlation between two genes was analyzed by Pearson statistics. The correlation of *FZD2* expression with survival was analyzed in the Kaplan–Meier plotter website (http://kmplot.com/analysis/).

Human Specimens

Forty-four BC specimens including 28 invasive ductal BC (IDC), 9 invasive lobular BC (ILC), and 7 ductal BC in situ (DCIS), and 10 matched cancer-adjacent normal tissues were investigated in this study. All these specimens were obtained from Liaoning Province Tumor Hospital with the informed consent of the patients. Institutional Research Ethics Committee of China Medical University approved the use of these specimens for research purposes.

Immunohistochemistry

Tissue sections were deparaffinized and hydrated, and then incubated with 3% H_2O_2 to remove endogenous peroxidase and treated with citrate buffer in heat to repair antigen. After incubation with primary antibody (Fzd2; 1:200; Abcam, Cambridge Science Park, UK) overnight at 4°C, biotinylated secondary antibody (1:1,000; Thermo Fisher Scientific, Waltham, MA, USA) was then added. Sections were stained with diaminobenzidine, and then restained in hematoxylin, dehydrated with gradient alcohol and xylene, and sealed with cover slides. Expression of Fzd2 in human BC tissues was assessed and scored by a clinical pathologist and a second investigator. Cells with no, faint, moderate, and strong staining were rated as 0, 1, 2, and 3, respectively. The percentage of corresponding staining cells was designated as A, B, C, and D, respectively. Expression score was calculated as 0×A + 1×B + 2×C + 3×D.

Cell Culture

MCF7, BT-549, and MDA-MB-231 were obtained from the American Type Culture Collection (ATCC), and MCF7/adriamycin (Adr) was purchased from icell-bioscience (Shanghai, China). MCF7, MDA-MB-231, and BT-549 cells were cultured in Dulbecco's modified Eagle's medium (DMEM) (Hyclone, Logan, UT, USA) containing 10% fetal bovine serum (FBS; MRC, New Zealand) and 1% penicillin/streptomycin (Hyclone). MCF7/Adr cells were maintained in RPMI-1640 medium supplemented with 10% FBS, 1% penicillin/streptomycin, and 1 μM Adr (Solarbio, Beijing, China). Doxorubicin was dissolved in pure water.

Western Blot

Equal amount of protein was separated by sodium dodecyl sulfate-polyacrylamide gel electrophoresis (SDS-PAGE) and transferred to polyvinylidene difluoride (PVDF) membranes. Bovine serum albumin (5%) or skimmed milk was performed to block membranes. Primary antibodies include Fzd2 and CD44 (1:5,000; Abcam); interleukin-6 (IL-6), Stat3, p-Stat3 (Tyr705), non-phospho β-catenin, E-cadherin, vimentin, Slug, Wnt5a/b, Yes-associated protein 1 (Yap1), TGF-β1, Smad3, and ABCG2 (1:1,000; Cell Signaling Technology, Boston, MA, USA); Wnt3, Col1a1, and Col6a1 (1:1,000; Abcam); Zeb1 (1:500; Sigma-Aldrich, St. Louis, MO, USA); and glyceraldehyde-3-phosphate dehydrogenase (GAPDH) (1:500; Proteintech, Chicago, IL, USA) were incubated with the membranes overnight. SuperSignal Chemiluminescent Substrates (Thermo Fisher Scientific) and imaging systems were used to analyze the results.

Coimmunoprecipitation (Co-IP)

Cell lysates were divided into two parts, and 2 μg of Fzd2 antibody (R&D Systems, Minneapolis, MN, USA) and 2 μg of mouse immunoglobulin G (IgG) antibody (Santa Cruz Biotechnology, Santa Cruz, CA, USA) were added, respectively. Protein A/G agarose beads (20 μl) (Santa Cruz Biotechnology) were added overnight. The agarose beads were then washed four times to clear the nonspecifically bound proteins. Protein buffer was added and Western blot was performed.

Cell Transfection

Three *FZD2* short hairpin RNA (shRNA) plasmids (sh1, sh2, and sh3; Genechem, Shanghai, China) were transiently transfected into 5×10^5 MDA-MB-231 cells and 5×10^5 BT-549 cells, respectively, with Lipofectamine 3000. *FZD2* shRNA (sh3) lentiviruses (Genechem) were transfected into 1×10^5 MDA-MB-231 cells, 1×10^5 BT-549 cells, and 1×10^5 MCF7/Adr cells, respectively, with HitransG P (Genechem) to stably knock down Fzd2 expression. Fzd2 stably knockdown (KD) cells were screened with puromycin. Target sequences were as follows: control sh: 5′-TTCTCCGAACGTGTCACGT-3′; sh1: 5′-caCCACGTACTTGGTAGACAT-3′; sh2: 5′-gcCCG ACTTCACGGTCTACAT-3′; and sh3: 5′-gcCATCCTAT CTCAGCTACAA-3′.

Immunofluorescence Assay

Cells were washed twice with phosphate-buffered saline (PBS) and fixed by 4% paraformaldehyde solution. Triton X-100 solution (1%) was added to penetrate the cytomembrane. Cells were then incubated with primary antibodies [E-cadherin (1:200), vimentin (1:100), and Slug (1:100), Cell Signaling Technology; Zeb1 (1:100), Sigma-Aldrich] for 2 h at 37°C, and a fluorescent secondary antibody (Alexa Fluor 488 and 594 donkey anti-rabbit IgG; 1:200; Invitrogen, Carlsbad, CA, USA) was added. The fluorescence was visualized by a confocal microscope (NIKON, Tokyo, Japan).

Migration and Invasion Assay

Wound healing assay was used to assess cell migration. In brief, cells were cultured in a six-well plate with 5×10^5 cells/well. The bottom of the plate was scratched with perpendicular straight lines. To evaluate cell invasion, 2×10^4 cells were seeded to the upper chambers of Transwell plates (Corning, Corning, NY, USA). In the lower chamber, 0.5 ml of medium with 10% FBS was added to promote cell movement. After 24 h, a cotton swab was used to clean the inside of the chamber. The migrated cells were fixed with a paraformaldehyde solution and stained with the crystal violet (Beyotime Biotechnology, Shanghai, China). Cells were determined in five randomly selected microscope fields.

Mammosphere Assay

MDA-MB-231 and MCF7/Adr cells were made into single cell suspensions and seeded in six-well Ultra-Low Attachment Surface Polystyrene culture plates (Corning) at a density of 1×10^4 cells/well. Then 2 ml MammoCult™ Human Medium kit (STEMCELL Technologies, Vancouver, Canada) was added into each well. The cells were incubated at 37°C and 5% CO_2 for 7 days. Mammospheres were counted in four randomly selected fields under an inverted microscope.

Flow Cytometry

Flow cytometry was used to determine $Lgr5^+$ cells. Cells were washed twice and resuspended with stain buffer (Invitrogen) and adjusted to 10^7 cells/ml. Five microliters of phycoerythrin (PE)-conjugated anti-hLgr5 (Invitrogen) antibody was added to each tube and incubated on ice for 30 min. Cells were washed twice again with stain buffer. BD Accuri C6 Plus (BD Biosciences; East Rutherford, NJ, USA) was used to detect and analyze the labeled cells.

MTT Assay

Cells were seeded in 96-well plates at a density of 5×10^3 cells/well. Cells were incubated with different concentrations of paclitaxel (Solarbio) for 48 h. MTT stain solution was added into the wells and incubated at 37°C for 4 h and then removed. Absorbance was measured at 570 nm. The formula of IC_{50} was as follow: $\lg IC_{50} = Xm\text{-}I\ (P\text{-}(3\text{-}Pm\text{-}Pn)/4)$.

Statistical Analysis

GraphPad Prism 7.0 (GraphPad Software Inc., San Diego, CA, USA) was performed to analyze the data, and all data were presented as the mean ± standard deviation (SD). Differences between two groups were assessed by Student *t*-test. A value of $p < 0.05$ is considered as significant.

RESULTS

Fzd2 Is Overexpressed in BC and Is Correlated With Unfavorable Prognosis

Immunohistochemistry was performed to examine Fzd2 protein expression in BC tissues. Fzd2 expression was extensively found in IDC (27/28), ILC (6/9), and DCIS (7/7) but was scarcely detected in cancer-adjacent normal tissues (3/10) (Fig. 1A and B). Expression scoring further revealed a higher expression level of Fzd2 in III + IV stage BC (Fig. 1C). TCGA database was interrogated for *FZD2* mRNA expression. Consistently, *FZD2* mRNA was overexpressed in IDC, ILC, mucinous BC, and metaplastic BC (MBC) (Fig. 1D). The relation of *FZD2* expression to survival was analyzed in a Kaplan–Meier plotter website[17]. High *FZD2* expression was associated with shortened overall survival (OS), relapse-free survival (RFS), and distant metastasis free survival (DMFS) (Fig. 1E).

Fzd2 Combines With and Modulates Wnt5a/b and Wnt3

The CCLE database was interrogated for mRNA expression of *FZD2* and some *Wnt* ligands[18] in a series of BC cell lines ($n = 57$). *FZD2* was positively correlated with *WNT5B* and *WNT3*, respectively (Fig. 2A). Similarly, interrogation of GSE12777 database showed that *FZD2* was correlated with *WNT5B* and *WNT3*, respectively, in another panel of BC cell lines ($n = 51$) (Fig. 2B). Interrogation of CCLE database further demonstrated that BC cell lines expressed a higher level of noncanonical *WNT5A* and *WNT5B* than canonical *WNT1* and *WNT3A* (Fig. 2C).

Fzd2 protein expression was determined in several chosen representative cell lines. Western blot detection showed that Fzd2 was strongly expressed in mesenchymal-like cell lines such as MDA-MB-231, Hs 578T, and BT-549, as well as a multidrug resistant cell line MCF7/Adr (Fig. 2D). Co-IP test confirmed the binding of Wnt5a/b and Wnt3 to Fzd2 in both MDA-MB-231 and BT-549 (Fig. 2E and F). To explore whether Fzd2 modulated Wnt5a/b and Wnt3, *FZD2* shRNA lentiviruses were used to transfect MDA-MB-231 and BT-549. As expected, Fzd2 KD significantly reduced Wnt5a/b and Wnt3 expression (Fig. 2G and H).

Fzd2 Maintains BC Cell Mesenchymal Phenotype

As Fzd2 was preferentially expressed in mesenchymal-like BC cells, we asked whether Fzd2 contributed to the mesenchymal phenotype of MDA-MB-231 and BT-549. Fzd2 KD reduced vimentin expression (Fig. 3A and B). Fzd2 KD also suppressed expression of EMT transcription factor (EMT-TF) Slug and Zeb1 (Fig. 3C and D). Moreover, Fzd2 KD decreased the expression of some mesenchymal-related proteins such as tenascin C (TNC)

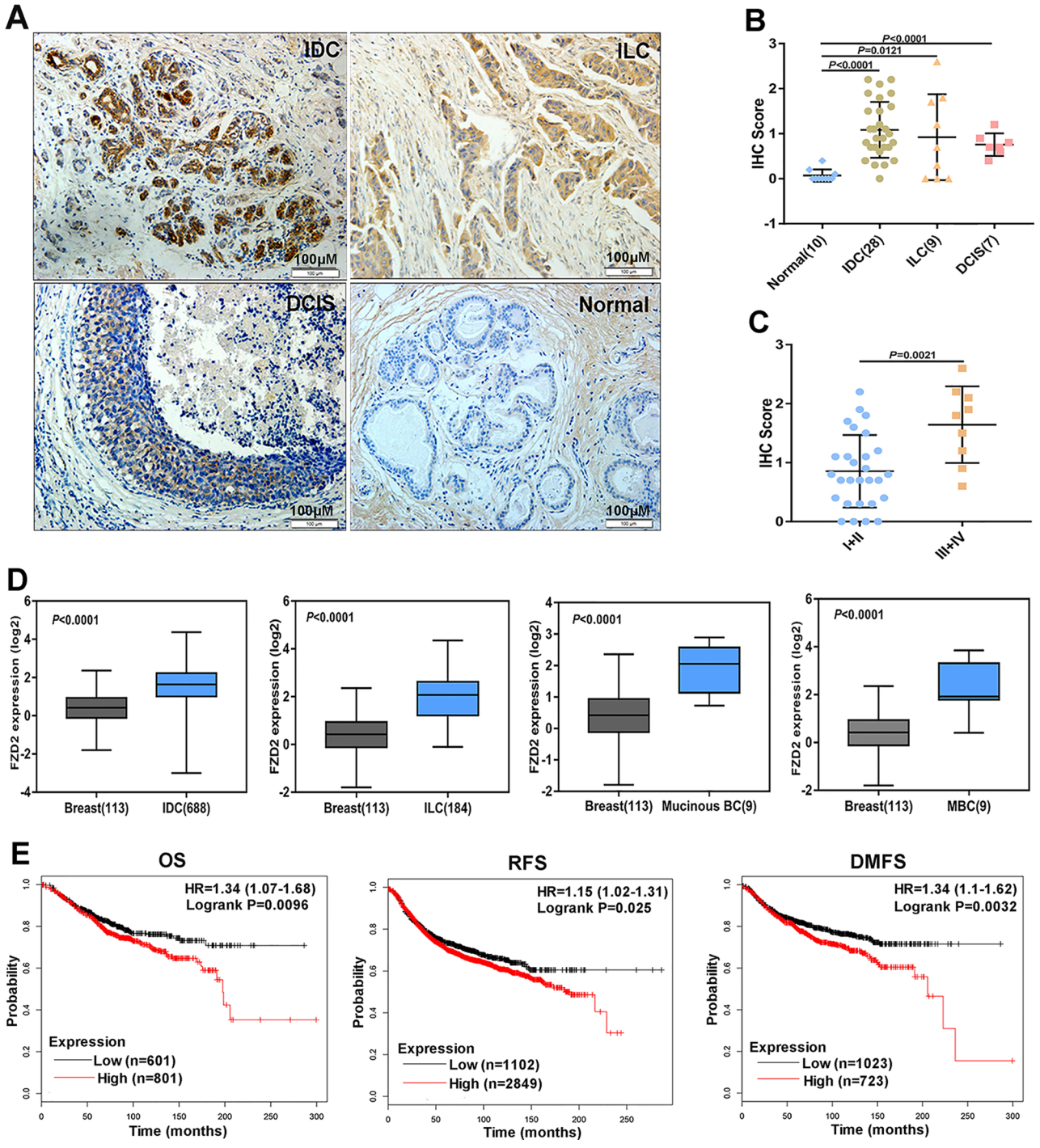

Figure 1. Frizzled 2 (Fzd2) is overexpressed in breast cancer and correlated with unfavorable prognosis. (A) Expression of Fzd2 in breast cancer (BC) tissues and cancer-adjacent normal tissues was detected by immunohistochemistry (IHC). (B) Expression of Fzd2 in cancer-adjacent normal tissues (Normal, $n = 10$), invasive ductal BC (IDC) ($n = 28$), invasive lobular BC (ILC) ($n = 9$), and ductal BC in situ (DCIS) ($n = 7$) was scored. Level of Fzd2 in IDC, ILC, and DCIS was compared to that in cancer-adjacent normal tissues, respectively. (C) Level of Fzd2 in I + II stage BC ($n = 28$) was compared to that in III + IV stage BC ($n = 9$). (D) The Cancer Genome Atlas (TCGA) database was interrogated for expression of *FZD2* mRNA. Level of FZD2 in IDC ($n = 688$), ILC ($n = 184$), mucinous BC ($n = 9$), and MBC ($n = 9$) was compared to that in normal breast, respectively. (E) Correlation of FZD2 expression with prognosis was analyzed in the Kaplan–Meier plotter website. Error bars indicate standard deviation (SD).

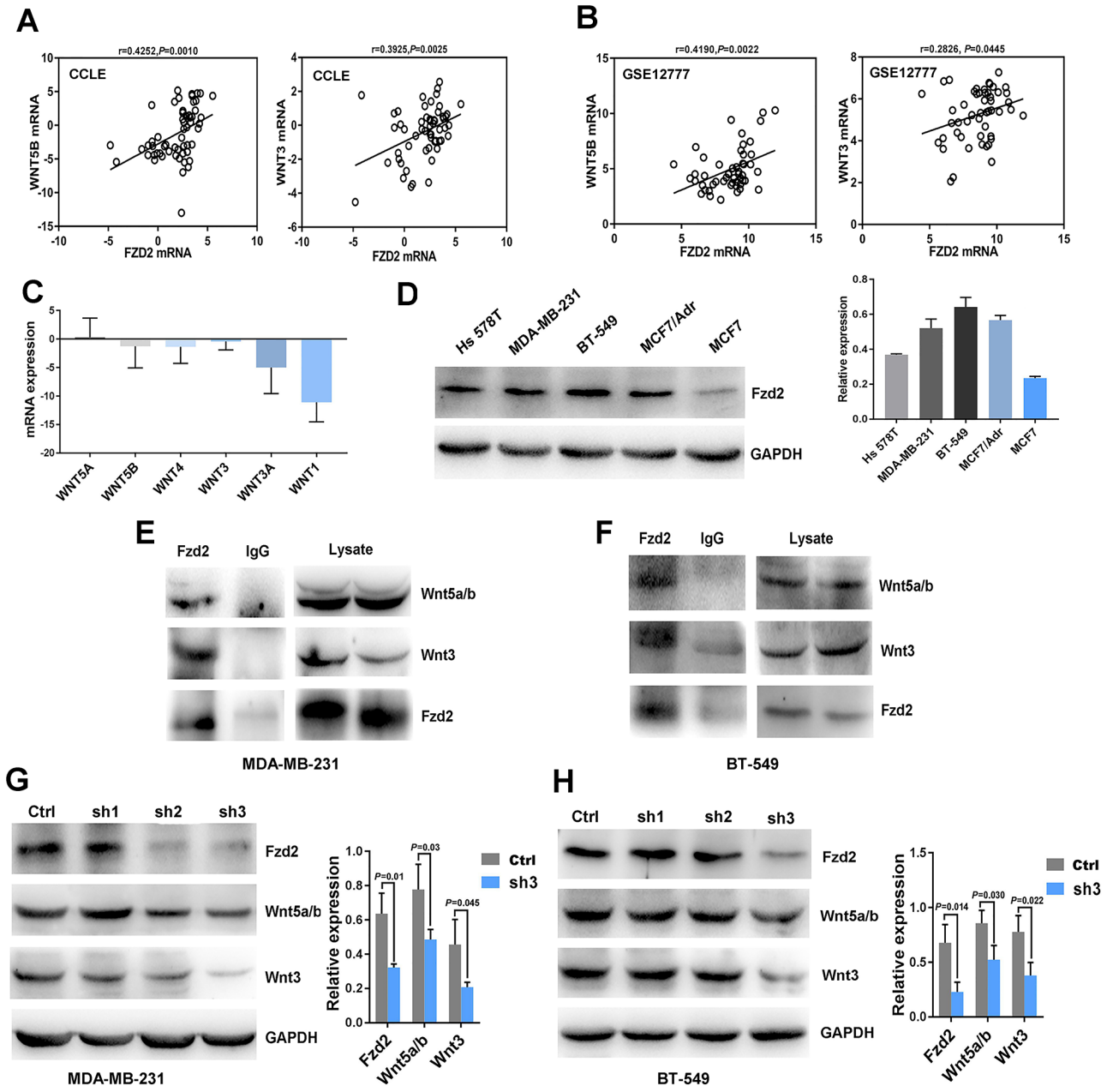

Figure 2. Fzd2 combines with and modulates Wnt5a/b and Wnt3. The CCLE database (A) and GSE12777 database (B) were interrogated for expression of *FZD2*, *WNT5B*, and *WNT3* mRNA in BC cell lines. Correlation between two genes was analyzed by Pearson statistics. (C) The CCLE database was interrogated for expression of several *WNT* in BC cell lines. Error bars indicate SD. (D) Expression of Fzd2 in several representative cell lines was detected by Western blot. Coimmunoprecipitation (Co-IP) test was performed to verify the binding of Wnt5a/b and Wnt3 to Fzd2 in MDA-MB-231 cells (E) and BT-549 cells (F). Expression of Fzd2, Wnt5a/b, and Wnt3 was detected by Western blot in MDA-MB-231 cells (G) and BT-549 cells (H), which were transfected with control short hairpin RNA (shRNA) (Ctrl) or *FZD2* shRNAs (sh1, sh2, and sh3). Error bars in (D), (G), and (H) indicate SD and are derived from three experiments.

and two collagens, Col1a1 and Col6a1 (Fig. 3E). These proteins have been implicated in BC metastasis and stemness[19–21]. Finally, Fzd2 KD inhibited BC cell migration and invasion (Fig. 3F and G) and induced an epithelial-like morphology in MDA-MB-231 (Fig. 3H).

Fzd2 Contributes to BC Cell Stemness

MDA-MB-231 and MCF7/Adr were chosen to investigate the relation of Fzd2 to BC cell stemness. Compared with MCF7, MCF7/Adr possessed

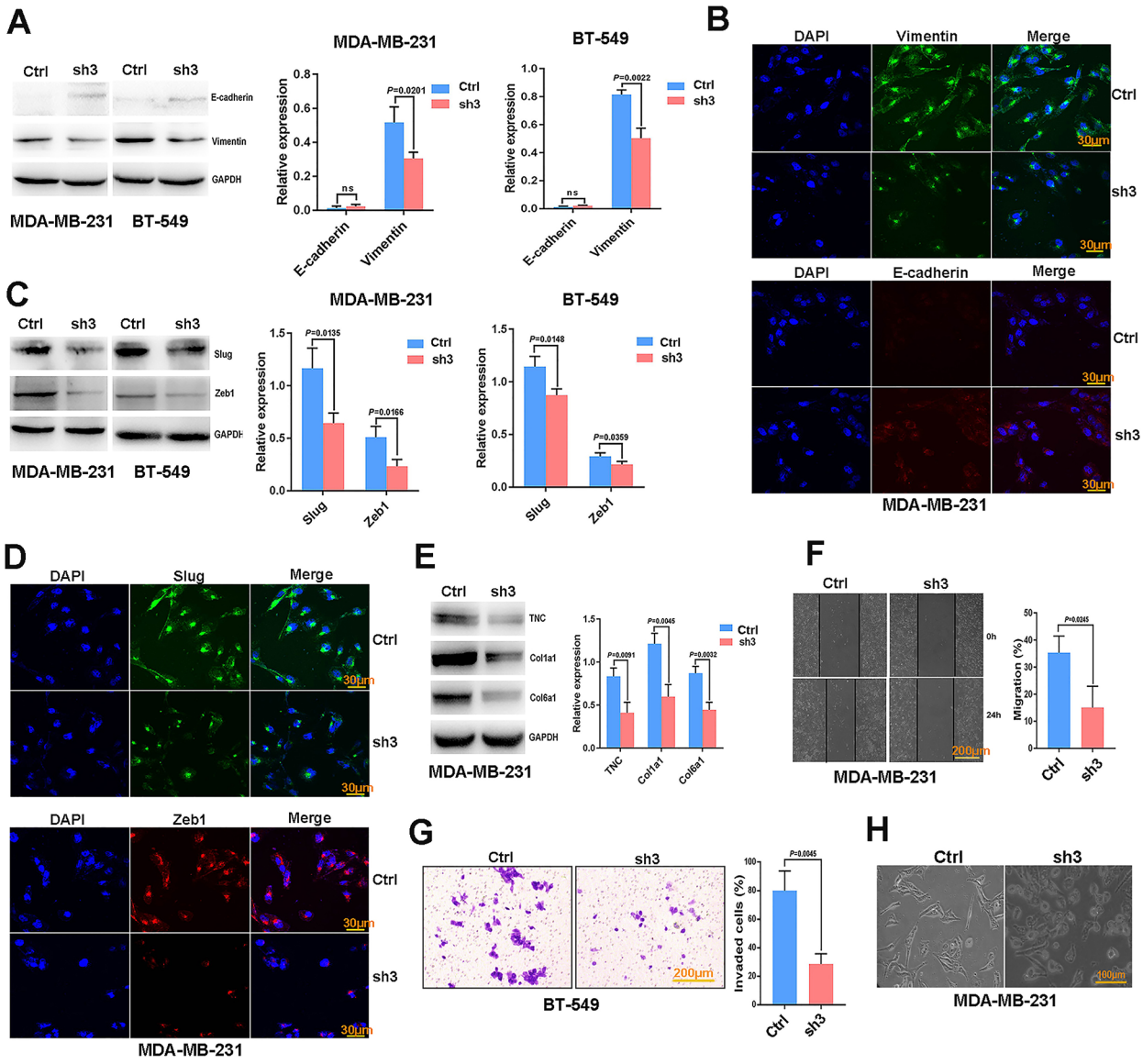

Figure 3. FZD2 maintains BC cell mesenchymal phenotype. (A) Expression of E-cadherin and vimentin in MDA-MB-231 cells and BT-549 cells transfected with control shRNA or *FZD2* sh3 was detected by Western blot. (B) Expression of E-cadherin and vimentin in MDA-MB-231 cells transfected with control shRNA or *FZD2* sh3 was detected by Immunofluorescence staining. (C) Expression of Slug and Zeb1 in MDA-MB-231 cells and BT-549 cells transfected with control shRNA or *FZD2* sh3 was detected by Western blot. (D) Expression of Slug and Zeb1 in MDA-MB-231 cells transfected with control shRNA or *FZD2* sh3 was detected by immunofluorescence staining. (E) Expression of TNC, Col1a1, and Col6a1 in MDA-MB-231 cells transfected with control shRNA or *FZD2* sh3 was detected by Western blot. (F) Migration of MDA-MB-231 cells transfected with control shRNA or *FZD2* sh3 was analyzed by wound healing test. (G) Invasion of BT-549 cells transfected with control shRNA or *FZD2* sh3 was analyzed by Transwell. (H) Morphological changes of MDA-MB-231 cells with control shRNA or *FZD2* sh3. Error bars indicate SD and are derived from three experiments.

mesenchymal traits and stemness[22]. Fzd2 KD impaired mammosphere formation capacity of these cells. Both sphere number and sphere size decreased significantly after Fzd2 KD (Fig. 4A and B). As leucine-rich repeat containing G protein coupled receptor 5 (Lgr5) is a potential marker of BC stem cells (BCSCs), the number of $Lgr5^+$ cells was quantified by flow cytometry. Fzd2 KD reduced the fraction of $Lgr5^+$ subpopulation (Fig. 4C and D). Furthermore, Fzd2 KD weakened CD44 expression (Fig. 4E). Notably, Fzd2 KD had no effect on the subpopulation of aldehyde dehydrogenase 1 positive ($ALDH1^+$) (data not shown). Interrogation of the CCLE database (Fig. 4F) and GSE12777 database (Fig. 4G) revealed that *FZD2* was positively correlated with

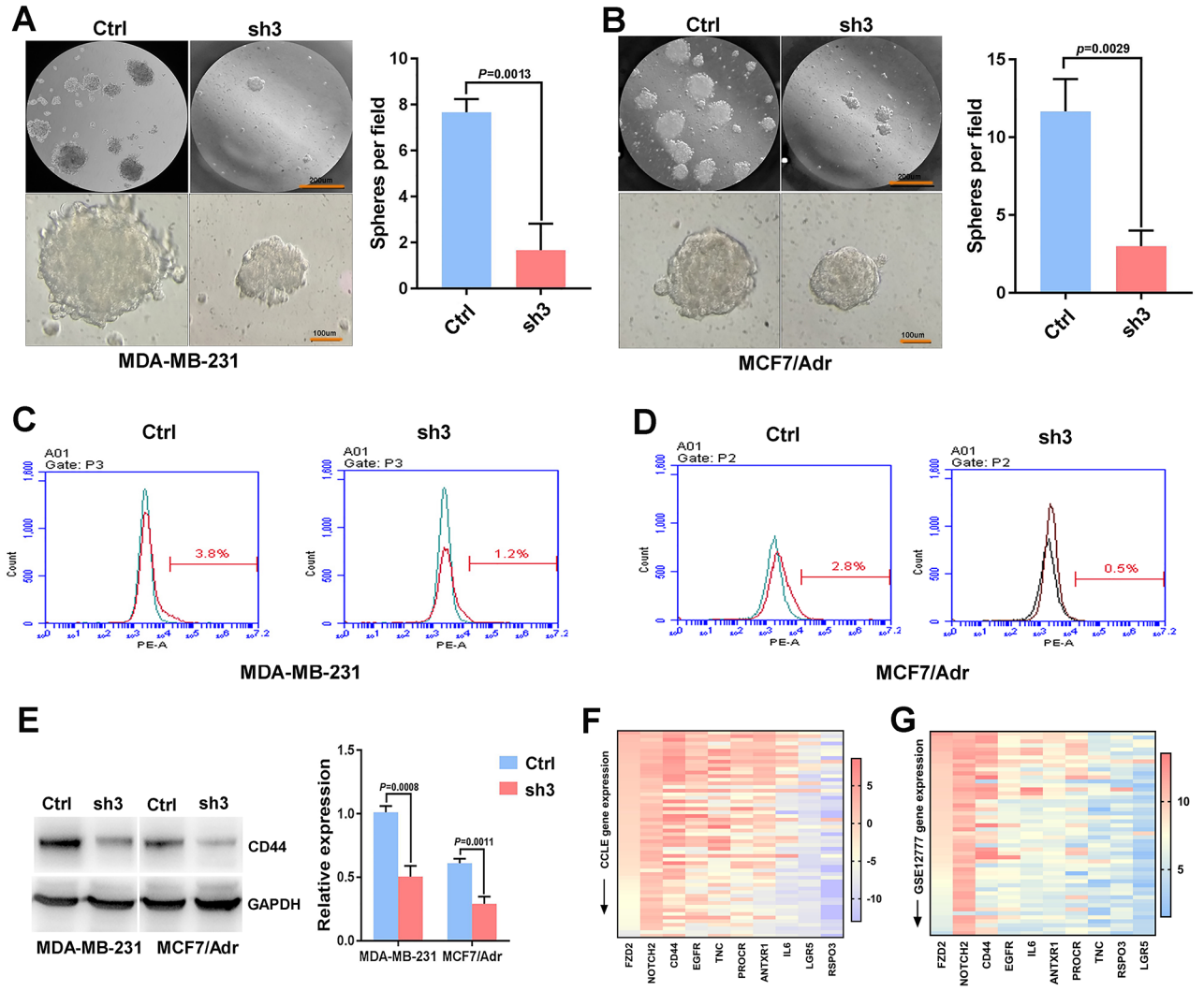

Figure 4. Fzd2 contributes to BC cell stemness. Mammosphere formation in MDA-MB-231 cells (A) and MCF7/Adr cells (B) transfected with control shRNA or *FZD2* sh3. The fraction of Lgr5$^+$ subpopulation in MDA-MB-231 cells (C) and MCF7/Adr cells (D) transfected with control shRNA or *FZD2* sh3 was determined by flow cytometry. (E) Expression of CD44 in MDA-MB-231 cells and BT-549 cells transfected with control shRNA or *FZD2* sh3 was detected by Western blot. Heat maps that were generated from the CCLE database (F) and GSE12777 (G) database demonstrated correlation of *FZD2* with some stemness-related genes. Error bars indicate SD and are derived from three experiments.

a series of stemness-related genes including *NOTCH2*, *EGFR*, *IL6*, *CD44*, *PROCR*, *LGR5*, *RSPO3*, *TNC*, and *ANTXR1*.

Fzd2 Cross-Talks With Several Oncogenic Pathways

The IL-6/Stat3 pathway is critical to the maintenance of mesenchymal-like stemness and the expansion of Lgr5$^+$ stem cells[23,24]. Wnt5a induces IL-6 expression in tumor and inflammation[25–27]. Based on these findings, relation of Fzd2 to IL-6/Stat3 was explored. Fzd2 KD reduced IL-6 expression and suppressed Stat3 phosphorylation in MDA-MB-231 and BT-549 (Fig. 5A and B). Yap1 mediates an oncogenic pathway in human cancers including BC, and Wnt5 stimulates the Yap1 pathway during development[28]. Accordingly, Fzd2 KD downregulated Yap1 expression in BC cells (Fig. 5A and B). Moreover, Fzd2 KD interfered with TGF-β1/Smad3 signaling (Fig. 5A and B). Expression of active β-catenin remained unchanged after Fzd2 KD, indicating Fzd2 signaling had no effect on the canonical Wnt/β-catenin pathway (Fig. 5A and B). Interrogation of the CCLE database (Fig. 5C, Table 1) and GSE12777 database (Fig. 5D, Table 2) further supported the cross-talk of Wnt/Fzd2 signaling with these pathways (Fig. 5E).

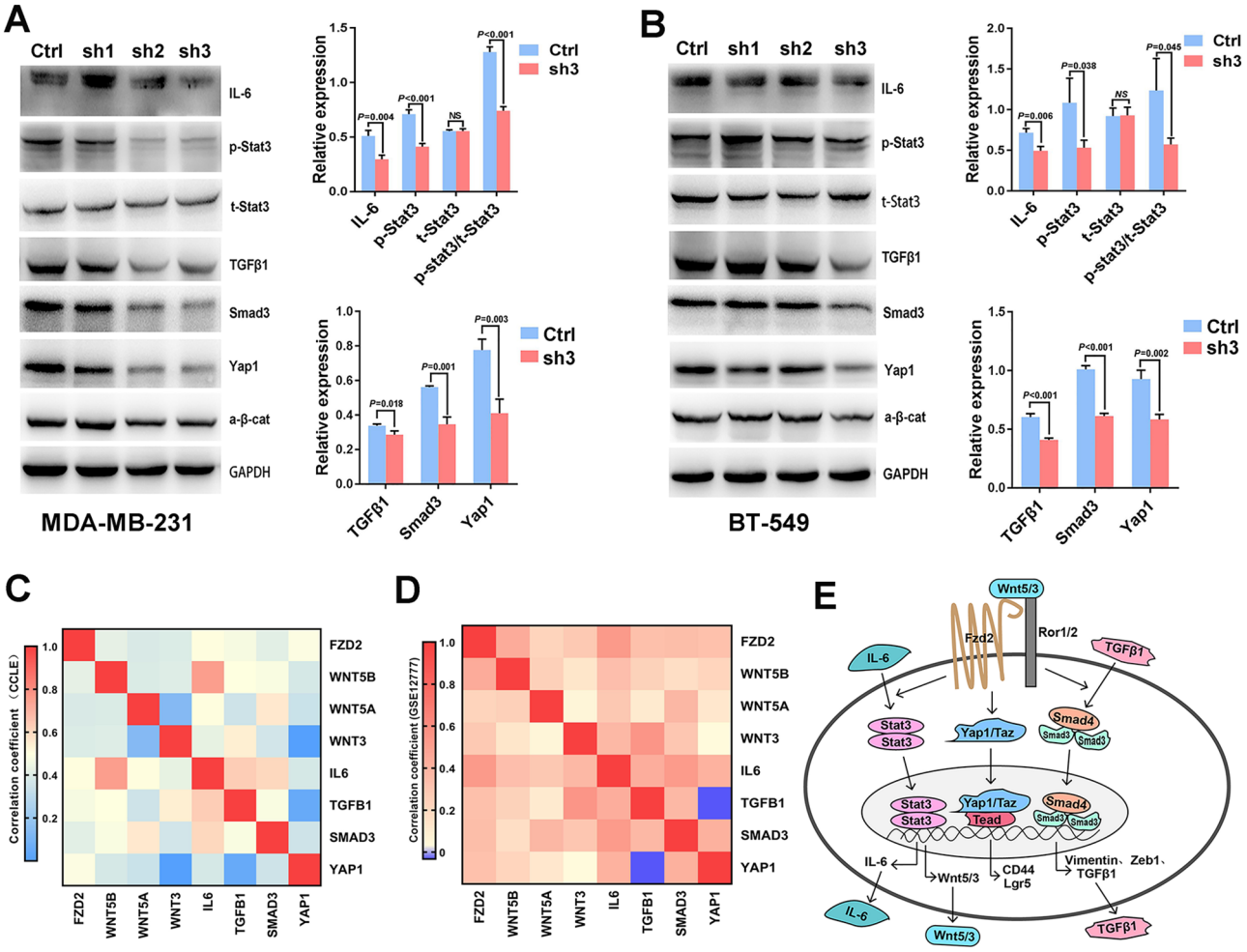

Figure 5. Fzd2 cross-talks with several oncogenic pathways. Expression of interleukin-6 (IL-6), p-Stat3, t-Stat3, transforming growth factor-β1 (TGF-β1), Smad3, Yes-associated protein 1 (Yap1), and active β-catenin (a-β-cat) in MDA-MB-231 cells (A) and BT-549 cells (B) transfected with control shRNA or *FZD2* shRNAs was detected by Western blot. Error bars indicate SD and are derived from three experiments. Heat maps generated from the CCLE database (C) and GSE12777 (D) database demonstrated the correlation of Wnt/Fzd2 signaling with other oncogenic pathways. (E) A schema indicates the cross-talk of Wnt/Fzd2 signaling with the IL-6/Stat3, TGFβ1/Smad3, and Yap1 pathways.

Table 1. *p* Values of Pearson Statistics [Cancer Cell Line Encyclopedia (CCLE) Database]

Gene	FZD2	WNT5B	WNT5A	WNT3	IL-6	TGFB1	SMAD3	YAP1
FZD2	0	0.001	0.0029	0.0025	7E-05	0.0002	0.0015	0.0001
WNT5B	0.001	0	0.0027	0.002	1E-11	9E-05	0.0002	0.0037
WNT5A	0.0029	0.0027	0	0.3214	7E-05	0.0075	7E-06	0.0099
WNT3	0.0025	0.002	0.3214	0	0.0009	1E-05	0.0053	0.9994
IL6	7E-05	1E-11	7E-05	0.0009	0	2E-07	8E-07	0.0039
TGFB1	0.0002	9E-05	0.0075	1E-05	2E-07	0	0.0001	0.7191
SMAD3	0.0015	0.0002	7E-06	0.0053	8E-07	0.0001	0	0.0071
YAP1	0.0001	0.0037	0.0099	0.9994	0.0039	0.7191	0.0071	0

CCLE database was interrogated for gene expression. Correlation between two genes was analyzed by Pearson statistics.

Table 2. *p* Values of Pearson Statistics (GSE12777 Database)

Gene	FZD2	WNT5B	WNT5A	WNT3	IL-6	TGFB1	SMAD3	YAP1
FZD2	0	0.0013	0.1249	0.0445	7E-05	0.0191	0.0142	0.021
WNT5B	0.0013	0	0.0875	0.3627	0.018	0.1029	0.2426	0.1329
WNT5A	0.1249	0.0875	0	0.7354	0.0434	0.4602	0.0071	0.3933
WNT3	0.0445	0.3627	0.7354	0	0.0076	3E-05	0.0361	0.8709
IL6	7E-05	0.018	0.0434	0.0076	0	0.002	8E-05	0.0035
TGFB1	0.0191	0.1029	0.4602	3E-05	0.002	0	0.0074	0.8174
SMAD3	0.0142	0.2426	0.0071	0.0361	8E-05	0.0074	0	0.003
YAP1	0.021	0.1329	0.3933	0.8709	0.0035	0.8174	0.003	0

GSE12777 database was interrogated for gene expression. Correlation between two genes was analyzed by Pearson statistics.

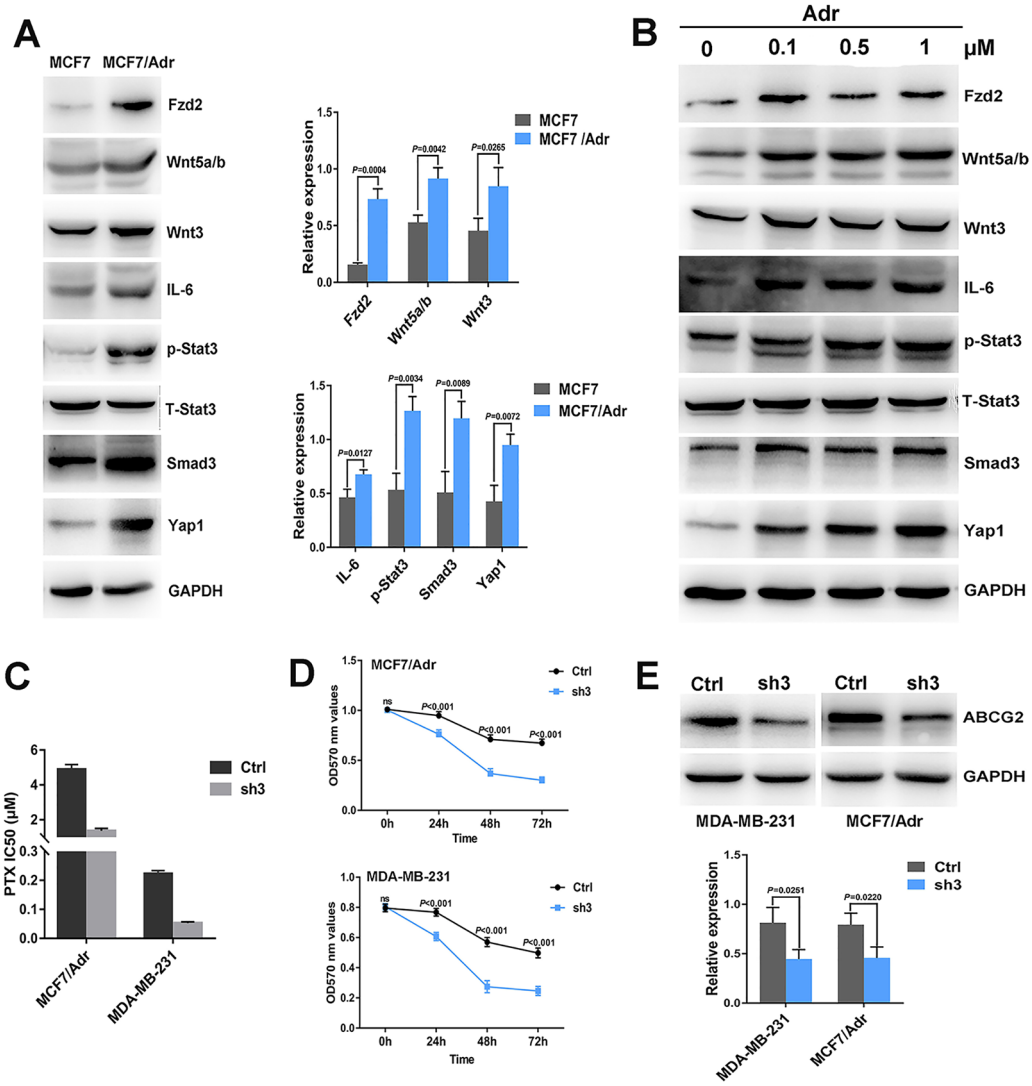

Figure 6. Fzd2 endows BC cell with drug resistance. (A) Expression of Fzd2, Wnt5a/b, Wnt3, IL-6, p-Stat3, t-Stat3, Smad3, and Yap1 in MCF7 cells and MCF7/Adr cells was detected by Western blot. (B) Expression of Fzd2, Wnt5a/b, Wnt3, IL-6, p-Stat3, t-Stat3, Smad3, and Yap1 in MCF7 cells treated with Adr (0.1, 0.5, and 1 μM, respectively) was detected by Western blot. (C) IC_{50} of paclitaxel (PTX) for MCF7/Adr cells and MDA-MB-231 cells transfected with control shRNA or *FZD2* sh3 was determined. (D) Viability of MCF7/Adr cells and MDA-MB-231 cells transfected with control shRNA or *FZD2* sh3 after PTX treatment for 48 h (3 and 0.1 μM, respectively) was determined by MTT. (E) Expression of ABCG2 in MDA-MB-231 cells and MCF7/Adr cells transfected with control shRNA or *FZD2* sh3 was detected by Western blot. Error bars indicate SD and are derived from three experiments.

Fzd2 Endows BC Cells With Drug Resistance

As shown in Figure 2D, Fzd2 expression was upregulated in MCF7/Adr, suggesting a potential role of Fzd2 in BC cell chemoresistance. MCF7/Adr expressed more Fzd2, Wnt5a/b, Wnt3, IL-6, p-Stat3, Yap1, and Smad3, compared with its parent MCF7 (Fig. 6A). Furthermore, treatment of MCF7 with Adr (0.1, 0.5, and 1 μM, respectively) for 24 h upregulated expression of these proteins (Fig. 6B). Fzd2 KD significantly lowered IC_{50} of paclitaxel (PTX) for both MCF7/Adr and MDA-MB-231 (Fig. 6C). Fzd2 KD enhanced the sensitivity of MCF7/Adr and MDA-MB-231 to PTX (3 and 0.1 μM, respectively) (Fig. 6D). ATP binding cassette subfamily G member 2 (ABCG2) plays crucial roles in drug resistance. Fzd2 KD remarkably reduced ABCG2 expression in MCF7/Adr and MDA-MB-231 (Fig. 6E).

DISCUSSION

Cancer stem cells (CSCs) are phenotypically heterogeneous and highly plastic. BCSCs exist in distinct EMT and MET states. Mesenchymal-like BCSCs are quiescent, characterized by $CD44^+CD24^-$, and localized at the tumor invasive front, while epithelial-like BCSCs are proliferative, characterized by $ALDH^+$, and localized more centrally[9]. The gene expression profiles of these two types of BCSCs resemble those of basal and luminal stem cells in normal breast, respectively[9]. In mouse, $CD29^{hi}CD61^+$ BCSCs exhibit mesenchymal-like abilities with high expression of EMT-associated genes, whereas $ALDH^+$ BCSCs are more closely related to luminal progenitors[29].

IL-6/Stat3 signaling is responsible for BC cell stemness[24,30,31]. Both cancer cells and stromal cells in the tumor microenvironment can produce IL-6. IL-6 from these cells promotes BC cell invasion, stemness, and drug resistance by activating Stat3. Actually, some BC cells secret IL-6 to induce Stat3 activation, which reversely promotes IL-6 secretion, forming a positive feedback loop to maintain consistent activation of this signaling[32,33]. Increasing evidence has indicated that IL-6/Stat3 is preferentially activated in $CD44^+CD24^-$ BCSCs, contributing to the mesenchymal-like stemness[13,24,32,33]. Stat3 inhibition decreased the expression of dormancy-associated genes and CSC-related genes, further demonstrating the role of Stat3 in mesenchymal-like CSCs[34]. Targeting the Stat3 pathway also reduced the tumor-initiating property of mouse $CD29^{hi}CD61^+$ BCSCs[29].

The Hippo pathway regulates Yap1 and affects tumorigenesis[35,36]. Studies have shown that Yap1 promotes BC growth, invasion, and metastasis[37–39]. Yap1 cross-talks with other oncogenic pathways. IL-6 mediates serum response factor (SRF)/Yap1-induced stemness[40]. TGF-β enhances Yap1 target gene expression or induces Yap1 activation[41–43]. Yap1 is significantly expressed in MMTV-WNT1 transgenic mice while not in MMTV-*βCATΔN* mice, indicating Wnt/β-catenin signaling has no effect on Yap1[28]. Intriguingly, in HEK293A cells, ectopic expression of Fzd2 alone could not induce Yap1 unless Ror1 was also expressed[28]. Moreover, Yap1 activation reversely induced Wnt5 secretion[28].

Lgr5 is a stem cell marker of various organs including the mammary gland[44]. $Lgr5^+$ CSCs have been identified in mouse intestinal adenomas and human colorectal cancer[45,46]. In BC, $Lgr5^+$ cells also display CSC-like traits[19,47]. Alternative to Wnt/β-catenin signaling, our study revealed that Fzd2-mediated noncanonical Wnt pathways are involved in the maintenance of $Lgr5^+$ cells. This was supported by CCLE analysis, which indicated that *FZD2* expression is correlated with *RSPO3* expression in BC cell lines. One recent study showed that *RSPO3* expression is correlated with *LGR5* expression, and Rspo3 KD inhibited BLBC EMT-like features, migration capacity, and tumor formation[48]. Furthermore, single-cell analysis demonstrated that early metastatic BC cells express high levels of EMT and stemness-associated genes, including *LGR5*[49].

ABCG2 is known as BC resistance protein (BCRP). As a drug efflux pump, ABCG2 plays crucial roles in chemoresistance. Moreover, ABCG2 is recognized as a CSC marker[50]. ABCG2 is regulated by the Wnt/β-catenin pathway in ovarian cancer and BC[51]. Our study revealed that the noncanonical Wnt/Fzd2 pathway induces chemoresistance via ABCG2. Inhibition of IL-6 and Smad3 was shown to downregulate ABCG2[52,53]. Consistently, CCLE analysis revealed a positive correlation of *ABCG2* with *WNT5B*, *SMAD3*, and *IL6*, respectively, in BC cell lines.

In summary, Fzd2 is implicated in a signaling network responsible for BC cell mesenchymal-like stemness. This network is initiated by Wnt5a/b and Wnt3, involving oncogenic pathways IL-6/Stat3, Yap1, and TGF-β1/Smad3. These pathways induce secretion of Wnt, IL-6, and TGF-β1 to form some positive autosustained loops (Fig. 5E). Via this network, Wnt/Fzd2 endows BC cells with mesenchymal-like stemness. Targeting Fzd2 may disrupt this signaling network and suppress BC metastasis, relapse, and drug resistance.

ACKNOWLEDGMENT: This work is supported by a grant from the Department of Science and Technology Liaoning Province (2017225028). The authors declare no conflicts of interest.

REFERENCES

1. Yin P, Wang W, Zhang Z, Bai Y, Gao J, Zhao C. Wnt signaling in human and mouse breast cancer: Focusing on Wnt ligands, receptors and antagonists. Cancer Sci. 2018;109(11):3368–75.
2. Chakrabarti R, Wei Y, Hwang J, Hang X, Andres Blanco M, Choudhury A, Tiede B, Romano RA, DeCoste C, Mercatali L, Ibrahim T, Amadori D, Kannan N, Eaves CJ, Sinha S,

Kang Y. DeltaNp63 promotes stem cell activity in mammary gland development and basal-like breast cancer by enhancing Fzd7 expression and Wnt signalling. Nat Cell Biol. 2014;16(10):1004–15.
3. DiMeo TA, Anderson K, Phadke P, Fan C, Perou CM, Naber S, Kuperwasser C. A novel lung metastasis signature links Wnt signaling with cancer cell self-renewal and epithelial–mesenchymal transition in basal-like breast cancer. Cancer Res. 2009;69(13):5364–73.
4. Wend P, Runke S, Wend K, Anchondo B, Yesayan M, Jardon M, Hardie N, Loddenkemper C, Ulasov I, Lesniak MS, Wolsky R, Bentolila LA, Grant SG, Elashoff D, Lehr S, Latimer JJ, Bose S, Sattar H, Krum SA, Miranda-Carboni GA. WNT10B/beta-catenin signalling induces HMGA2 and proliferation in metastatic triple-negative breast cancer. EMBO Mol Med. 2013;5(2):264–79.
5. Han B, Zhou B, Qu Y, Gao B, Xu Y, Chung S, Tanaka H, Yang W, Giuliano AE, Cui X. FOXC1-induced non-canonical WNT5A-MMP7 signaling regulates invasiveness in triple-negative breast cancer. Oncogene 2018;37(10):1399–408.
6. Safholm A, Tuomela J, Rosenkvist J, Dejmek J, Harkonen P, Andersson T. The Wnt-5a-derived hexapeptide Foxy-5 inhibits breast cancer metastasis in vivo by targeting cell motility. Clin Cancer Res. 2008;14(20):6556–63.
7. Mikels AJ, Nusse R. Purified Wnt5a protein activates or inhibits beta-catenin-TCF signaling depending on receptor context. PLoS Biol. 2006;4(4):e115.
8. Sato A, Yamamoto H, Sakane H, Koyama H, Kikuchi A. Wnt5a regulates distinct signalling pathways by binding to Frizzled2. EMBO J. 2010;29(1):41–54.
9. Liu S, Cong Y, Wang D, Sun Y, Deng L, Liu Y, Martin-Trevino R, Shang L, McDermott SP, Landis MD, Hong S, Adams A, D'Angelo R, Ginestier C, Charafe-Jauffret E, Clouthier SG, Birnbaum D, Wong ST, Zhan M, Chang JC, Wicha MS. Breast cancer stem cells transition between epithelial and mesenchymal states reflective of their normal counterparts. Stem Cell Reports 2014;2(1):78–91.
10. Fantozzi A, Gruber DC, Pisarsky L, Heck C, Kunita A, Yilmaz M, Meyer-Schaller N, Cornille K, Hopfer U, Bentires-Alj M, Christofori G. VEGF-mediated angiogenesis links EMT-induced cancer stemness to tumor initiation. Cancer Res. 2014;74(5):1566–75.
11. Guen VJ, Chavarria TE, Kroger C, Ye X, Weinberg RA, Lees JA. EMT programs promote basal mammary stem cell and tumor-initiating cell stemness by inducing primary ciliogenesis and Hedgehog signaling. Proc Natl Acad Sci USA 2017;114(49):E10532–9.
12. Herschkowitz JI, Zhao W, Zhang M, Usary J, Murrow G, Edwards D, Knezevic J, Greene SB, Darr D, Troester MA, Hilsenbeck SG, Medina D, Perou CM, Rosen JM. Comparative oncogenomics identifies breast tumors enriched in functional tumor-initiating cells. Proc Natl Acad Sci USA 2012;109(8):2778–83.
13. Woosley AN, Dalton AC, Hussey GS, Howley BV, Mohanty BK, Grelet S, Dincman T, Bloos S. TGFbeta promotes breast cancer stem cell self-renewal through an ILEI/LIFR signaling axis. Oncogene 2019;38(20):3794–811.
14. Morel AP, Hinkal GW, Thomas C, Fauvet F, Courtois-Cox S, Wierinckx A, Devouassoux-Shisheboran M, Treilleux I, Tissier A, Gras B, Pourchet J, Puisieux I, Browne GJ, Spicer DB, Lachuer J, Ansieau S, Puisieux A. EMT inducers catalyze malignant transformation of mammary epithelial cells and drive tumorigenesis towards claudin-low tumors in transgenic mice. PLoS Genet. 2012;8(5):e1002723.
15. Yang L, Wu X, Wang Y, Zhang K, Wu J, Yuan YC, Deng X, Chen L, Kim CC, Lau S, Somlo G, Yen Y. FZD7 has a critical role in cell proliferation in triple negative breast cancer. Oncogene 2011;30(43):4437–46.
16. Corda G, Sala G, Lattanzio R, Iezzi M, Sallese M, Fragassi G, Lamolinara A, Mirza H, Barcaroli D, Ermler S, Silva E, Yasaei H, Newbold RF, Vagnarelli P, Mottolese M, Natali PG, Perracchio L, Quist J, Grigoriadis A, Marra P, Tutt AN, Piantelli M, Iacobelli S, De Laurenzi V, Sala A. Functional and prognostic significance of the genomic amplification of frizzled 6 (FZD6) in breast cancer. J Pathol. 2017;241(3):350–61.
17. Lanczky A, Nagy A, Bottai G, Munkacsy G, Szabo A, Santarpia L, Gyorffy B. miRpower: A web-tool to validate survival-associated miRNAs utilizing expression data from 2178 breast cancer patients. Breast Cancer Res Treat. 2016;160(3):439–46.
18. Dijksterhuis JP, Baljinnyam B, Stanger K, Sercan HO, Ji Y, Andres O, Rubin JS, Hannoush RN, Schulte G. Systematic mapping of WNT-FZD protein interactions reveals functional selectivity by distinct WNT–FZD pairs. J Biol Chem. 2015;290(11):6789–98.
19. Oskarsson T, Acharyya S, Zhang XH, Vanharanta S, Tavazoie SF, Morris PG, Downey RJ, Manova-Todorova K, Brogi E, Massague J. Breast cancer cells produce tenascin C as a metastatic niche component to colonize the lungs. Nat Med. 2011;17(7):867–74.
20. Chen D, Bhat-Nakshatri P, Goswami C, Badve S, Nakshatri H. ANTXR1, a stem cell-enriched functional biomarker, connects collagen signaling to cancer stem-like cells and metastasis in breast cancer. Cancer Res. 2013;73(18):5821–33.
21. Gao H, Chakraborty G, Zhang Z, Akalay I, Gadiya M, Gao Y, Sinha S, Hu J, Jiang C, Akram M, Brogi E, Leitinger B, Giancotti FG. Multi-organ site metastatic reactivation mediated by non-canonical discoidin domain receptor 1 signaling. Cell 2016;166(1):47–62.
22. Calcagno AM, Salcido CD, Gillet JP, Wu CP, Fostel JM, Mumau MD, Gottesman MM, Varticovski L, Ambudkar SV. Prolonged drug selection of breast cancer cells and enrichment of cancer stem cell characteristics. J Natl Cancer Inst. 2010;102(21):1637–52.
23. Lindemans CA, Calafiore M, Mertelsmann AM, O'Connor MH, Dudakov JA, Jenq RR, Velardi E, Young LF, Smith OM, Lawrence G, Ivanov JA, Fu YY, Takashima S, Hua G, Martin ML, O'Rourke KP, Lo YH, Mokry M, Romera-Hernandez M, Cupedo T, Dow L, Nieuwenhuis EE, Shroyer NF, Liu C, Kolesnick R, van den Brink MRM, Hanash AM. Interleukin-22 promotes intestinal-stem-cell-mediated epithelial regeneration. Nature 2015;528(7583):560–4.
24. Marotta LL, Almendro V, Marusyk A, Shipitsin M, Schemme J, Walker SR, Bloushtain-Qimron N, Kim JJ, Choudhury SA, Maruyama R, Wu Z, Gonen M, Mulvey LA, Bessarabova MO, Huh SJ, Silver SJ, Kim SY, Park SY, Lee HE, Anderson KS, Richardson AL, Nikolskaya T, Nikolsky Y, Liu XS, Root DE, Hahn WC, Frank DA, Polyak K. The JAK2/STAT3 signaling pathway is required for growth of CD44(+)CD24(-) stem cell-like breast cancer cells in human tumors. J Clin Invest. 2011;121(7):2723–35.
25. Chen D, Li G, Fu X, Li P, Zhang J, Luo L. Wnt5a deficiency regulates inflammatory cytokine secretion, polarization, and apoptosis in mycobacterium tuberculosis-infected macrophages. DNA Cell Biol. 2017;36(1):58–66.
26. Fuster JJ, Zuriaga MA, Ngo DT, Farb MG, Aprahamian T, Yamaguchi TP, Gokce N, Walsh K. Noncanonical Wnt

signaling promotes obesity-induced adipose tissue inflammation and metabolic dysfunction independent of adipose tissue expansion. Diabetes 2015;64(4):1235–48.
27. Linnskog R, Mohapatra P, Moradi F, Prasad CP, Andersson T. Demonstration of a WNT5A-IL-6 positive feedback loop in melanoma cells: Dual interference of this loop more effectively impairs melanoma cell invasion. Oncotarget 2016;7(25):37790–802.
28. Park HW, Kim YC, Yu B, Moroishi T, Mo JS, Plouffe SW, Meng Z, Lin KC, Yu FX, Alexander CM, Wang CY, Guan KL. Alternative Wnt signaling activates YAP/TAZ. Cell 2015;162(4):780–94.
29. Yeo SK, Wen J, Chen S, Guan JL. Autophagy differentially regulates distinct breast cancer stem-like cells in murine models via EGFR/Stat3 and Tgfbeta/Smad signaling. Cancer Res. 2016;76(11):3397–410.
30. Wang T, Fahrmann JF, Lee H, Li YJ, Tripathi SC, Yue C, Zhang C, Lifshitz V, Song J, Yuan Y, Somlo G, Jandial R, Ann D, Hanash S, Jove R, Yu H. JAK/STAT3-regulated fatty acid beta-oxidation is critical for breast cancer stem cell self-renewal and chemoresistance. Cell Metab. 2018;27(1):136–50.e5.
31. Wei W, Tweardy DJ, Zhang M, Zhang X, Landua J, Petrovic I, Bu W, Roarty K, Hilsenbeck SG, Rosen JM, Lewis MT. STAT3 signaling is activated preferentially in tumor-initiating cells in claudin-low models of human breast cancer. Stem Cells 2014;32(10):2571–82.
32. Lambert AW, Wong CK, Ozturk S, Papageorgis P, Raghunathan R, Alekseyev Y, Gower AC, Reinhard BM, Abdolmaleky HM, Thiagalingam S. Tumor cell-derived periostin regulates cytokines that maintain breast cancer stem cells. Mol Cancer Res. 2016;14(1):103–13.
33. Lan J, Lu H, Samanta D, Salman S, Lu Y, Semenza GL. Hypoxia-inducible factor 1-dependent expression of adenosine receptor 2B promotes breast cancer stem cell enrichment. Proc Natl Acad Sci USA 2018;115(41):E9640–8.
34. Johnson RW, Finger EC, Olcina MM, Vilalta M, Aguilera T, Miao Y, Merkel AR, Johnson JR, Sterling JA, Wu JY, Giaccia AJ. Induction of LIFR confers a dormancy phenotype in breast cancer cells disseminated to the bone marrow. Nat Cell Biol. 2016;18(10):1078–89.
35. Dethlefsen C, Hansen LS, Lillelund C, Andersen C, Gehl J, Christensen JF, Pedersen BK, Hojman P. Exercise-induced catecholamines activate the hippo tumor suppressor pathway to reduce risks of breast cancer development. Cancer Res. 2017;77(18):4894–904.
36. Si Y, Ji X, Cao X, Dai X, Xu L, Zhao H, Guo X, Yan H, Zhang H, Zhu C, Zhou Q, Tang M, Xia Z, Li L, Cong YS, Ye S, Liang T, Feng XH, Zhao B. Src inhibits the hippo tumor suppressor pathway through tyrosine phosphorylation of Lats1. Cancer Res. 2017;77(18):4868–80.
37. Chen D, Sun Y, Wei Y, Zhang P, Rezaeian AH, Teruya-Feldstein J, Gupta S, Liang H, Lin HK, Hung MC, Ma L. LIFR is a breast cancer metastasis suppressor upstream of the Hippo–YAP pathway and a prognostic marker. Nat Med. 2012;18(10):1511–7.
38. Lamar JM, Stern P, Liu H, Schindler JW, Jiang ZG, Hynes RO. The Hippo pathway target, YAP, promotes metastasis through its TEAD-interaction domain. Proc Natl Acad Sci USA 2012;109(37):E2441–50.
39. Zanconato F, Forcato M, Battilana G, Azzolin L, Quaranta E, Bodega B, Rosato A, Bicciato S, Cordenonsi M, Piccolo S. Genome-wide association between YAP/TAZ/TEAD and AP-1 at enhancers drives oncogenic growth. Nat Cell Biol. 2015;17(9):1218–27.
40. Kim T, Yang SJ, Hwang D, Song J, Kim M, Kyum Kim S, Kang K, Ahn J, Lee D, Kim MY, Kim S, Seung Koo J, Seok Koh S, Kim SY, Lim DS. A basal-like breast cancer-specific role for SRF-IL6 in YAP-induced cancer stemness. Nat Commun. 2015;6:10186.
41. Ma B, Cheng H, Gao R, Mu C, Chen L, Wu S, Chen Q, Zhu Y. Zyxin–Siah2–Lats2 axis mediates cooperation between Hippo and TGF-beta signalling pathways. Nat Commun. 2016;7:11123.
42. Pefani DE, Pankova D, Abraham AG, Grawenda AM, Vlahov N, Scrace S, E ON. TGF-beta targets the Hippo pathway scaffold RASSF1A to facilitate YAP/SMAD2 nuclear translocation. Mol Cell 2016;63(1):156–66.
43. Lehmann W, Mossmann D, Kleemann J, Mock K, Meisinger C, Brummer T, Herr R, Brabletz S, Stemmler MP, Brabletz T. ZEB1 turns into a transcriptional activator by interacting with YAP1 in aggressive cancer types. Nat Commun. 2016;7:10498.
44. Leung C, Tan SH, Barker N. Recent advances in Lgr5(+) stem cell research. Trends Cell Biol. 2018;28(5):380–91.
45. Schepers AG, Snippert HJ, Stange DE, van den Born M, van Es JH, van de Wetering M, Clevers H. Lineage tracing reveals Lgr5+ stem cell activity in mouse intestinal adenomas. Science 2012;337(6095):730–5.
46. Shimokawa M, Ohta Y, Nishikori S, Matano M, Takano A, Fujii M, Date S, Sugimoto S, Kanai T, Sato T. Visualization and targeting of LGR5(+) human colon cancer stem cells. Nature 2017;545(7653):187–92.
47. Koren S, Reavie L, Couto JP, De Silva D, Stadler MB, Roloff T, Britschgi A, Eichlisberger T, Kohler H, Aina O, Cardiff RD, Bentires-Alj M. PIK3CA(H1047R) induces multipotency and multi-lineage mammary tumours. Nature 2015;525(7567):114–8.
48. Tocci JM, Felcher CM, Garcia Sola ME, Goddio MV, Zimberlin MN, Rubinstein N, Srebrow A, Coso OA, Abba MC, Meiss RP, Kordon EC. R-spondin3 is associated with basal-progenitor behavior in normal and tumor mammary cells. Cancer Res. 2018;78(16):4497–511.
49. Lawson DA, Bhakta NR, Kessenbrock K, Prummel KD, Yu Y, Takai K, Zhou A, Eyob H, Balakrishnan S, Wang CY, Yaswen P, Goga A, Werb Z. Single-cell analysis reveals a stem-cell program in human metastatic breast cancer cells. Nature 2015;526(7571):131–5.
50. Westover D, Li F. New trends for overcoming ABCG2/BCRP-mediated resistance to cancer therapies. J Exp Clin Cancer Res. 2015;34:159.
51. Chau WK, Ip CK, Mak AS, Lai HC, Wong AS. c-Kit mediates chemoresistance and tumor-initiating capacity of ovarian cancer cells through activation of Wnt/beta-catenin-ATP-binding cassette G2 signaling. Oncogene 2013;32(22):2767–81.
52. DiNatale BC, Smith K, John K, Krishnegowda G, Amin SG, Perdew GH. Ah receptor antagonism represses head and neck tumor cell aggressive phenotype. Mol Cancer Res. 2012;10(10):1369–79.
53. Wu CP, Murakami M, Hsiao SH, Liu TC, Yeh N, Li YQ, Hung TH, Wu YS, Ambudkar SV. SIS3, a specific inhibitor of Smad3 reverses ABCB1- and ABCG2-mediated multidrug resistance in cancer cell lines. Cancer Lett. 2018;433:259–72.